ARTERIAL BLOOD PRESSURE WAVEFORM ARTIFACTS DETECTION USING SHORT-TIME FOURIER TRANSFORM

Valeriia Trukhan[1], Josef Skola[1,2], Lenka Horakova[1,2,3], Martin Rozanek[1]

[1]Department of Biomedical Technology, Faculty of Biomedical Engineering, Czech Technical University in Prague, Kladno, Czech Republic

[2]Department of Anaesthesiology and Critical Care, Bulovka University Hospital, Prague, Czech Republic

[3]Department of Anaesthesiology, Perioperative and Intensive Care Medicine, Faculty of Health Studies, J. E. Purkyne University in Usti nad Labem and Krajska zdravotni, a. s., Masaryk Hospital, Usti nad Labem, Czech Republic

Abstract

High-frequency waveform recordings of biological signals enable more detailed data analysis and deeper physiological exploration. However, the waveform data—like invasive arterial blood pressure (ABP)—are particularly susceptible to frequent contamination with artifacts that can devalue the subsequent calculations like pressure reactivity index (PRx). This study aimed to verify the ability of the short-time Fourier transform (STFT) based algorithm to detect artifacts in the ABP waveform. Four types of modeled artifacts (rectangular, fast impulse, sawtooth and baseline drift) with different durations and amplitudes were inserted into undisturbed ABP waveforms. Short-time Fourier transform with a 5-second time window is computed on artifact-polluted ABP signals to detect changes in the frequency domain caused by these artifacts. An algorithm with three decision-making rules based on the dominant frequency component, standardized power spectrum, and the value of the second harmonic of the dominant frequency was used. Only segments that passed all three rules were labeled as artifact-free. Results indicated high sensitivity (93.35% and 94.83%) in detecting rectangular and sawtooth artifacts, with specificity exceeding 99% for both. Baseline drift artifact was detected with a low sensitivity of 5.02%, and fast impulse was not detected. This study proposes the application of a short-time Fourier transform-based algorithm to enhance the detection of clinically significant artifacts in arterial blood pressure signals, particularly relevant for PRx and other secondary calculations.

Keywords

artifacts, data cleaning, invasive blood pressure measurement, monitoring error, pressure reactivity index, short-time Fourier transform, signal processing, waveform

Introduction

The availability of high-frequency recording of biological signals opens an opportunity to perform various secondary calculations and analyses to explore the underlying physiology. Still, the noisiness and artifacts in the source signals could compromise these calculations. This problem is particularly pronounced in neurointensive care multimodal monitoring [1]. A frequently used parameter for assessing cerebrovascular autoregulation in traumatic brain injury patients is the pressure reactivity index (PRx). This index is calculated by taking the Pearson's correlation coefficient—a statistical measure of how two variables move together—between arterial blood pressure (ABP) and intracranial pressure (ICP) over a moving time window [2]. This means that the relationship between ABP and ICP is continuously monitored and analyzed in small time segments, allowing for an ongoing assessment of how changes in blood pressure relate to changes in intracranial pressure. PRx can be significantly compromised by the presence of artifacts in the arterial blood pressure, intracranial pressure, or both signals. A single arterial line flush artifact can significantly affect 8.3% of PRx values in the given hour [3].

Arterial blood pressure waveform, used besides other analyses for PRx calculation, is susceptible to artifacts arising from the measurement line, caused by air

Lekar a technika – Clinician and Technology 2024, vol. 54(2), pp. 63–72, DOI: 10.14311/CTJ.2024.2.05
ISSN 0301-5491 (Print), ISSN 2336-5552 (Online)

bubbles or blood clots in the fluid-filled tube, mechanical vibrations transmitted to the pressure transducer (e.g., patient movements, rubbing a cloth over the measuring system), or tube constriction between the catheter and transducer (due to crimping, during proximal blood pressure cuff inflation, etc.) [4–6]. Furthermore, daily care like line flushing and blood sampling regularly adds artifacts [7, 8].

Several approaches to automated identification and artifact removal from the ABP signal have already been published (reviewed in [9]). Some studies have focused on artifacts in numerical values, using averaged ABP [10, 11] and mean arterial pressure (MAP) values [9, 12]. The entire waveform has been analyzed with machine learning techniques and algorithms from image analysis [8, 11, 13, 14], time series [5], and signal abnormality analysis [15, 16]. While machine learning-based tools offer new solutions, they demand significant processing time and extensive training datasets annotated by experienced researchers or physicians. The choice of algorithm depends on the analysis's time scale; offline post-hoc analysis tolerates longer processing times and false positives, whereas real-time bedside calculations require simpler, less computationally intensive algorithms [8].

This study aims to verify the effectiveness of a short-time Fourier transform-based algorithm in detecting four modeled artifacts in arterial blood pressure waveforms, with the goal of improving the reliability of PRx index calculations.

Methods

Type of study

We conducted a retrospective analysis of high-frequency multimodal monitoring data from a fully anonymized critical care database, with no available patient identifiers. All methods were performed in accordance with the relevant guidelines and regulations.

Data

The data were recorded in the Neurointensive Care Unit of the Department of Anesthesiology, Perioperative Medicine and Intensive Care, Masaryk Hospital in Usti nad Labem, Czech Republic. All patients in the database had continuous synchronized data collected via ICM+ software (version 8.6, Cambridge Enterprise Ltd., Cambridge, UK). Arterial blood pressure was monitored by Carescape B850 vital signs monitor (GE Healthcare, Helsinki, Finland) and sampled at 200 Hz. The datasets for this study contained only arterial blood pressure data; no patient characteristics—such as sex, age, date of admission, diagnosis, or outcome—were available.

From a database with anonymized arterial blood pressure waveforms, two clinicians in agreement identified undisturbed ABP waveforms without apparent artifacts, with MAP of 90±5 mmHg and without apparent arrhythmias. From these waveforms, 20 segments of 10 minutes in length each were randomly selected, a total of 200 minutes. Each segment was then divided into four 2.5-minute parts. Thus, the final dataset consisted of 80 segments of 2.5 minutes. The dataset did not include any patient information, even the number of segments per patient.

Data analysis and artifact identification

Four types of simulated artifacts (rectangular, fast impulse, sawtooth and baseline drift) with different lengths and amplitudes (Table 1, Fig. 1) were inserted into each of the 80 undisturbed segments of the ABP waveform (at 4th second). Thirty-five different artifacts were inserted into each segment; thus 2800 analyses were performed. The modeling of each artifact's duration and amplitude was based on the characteristics observed in the native raw data recorded in critical care patients and published previously [3] and performed in MATLAB software (version R2020a, MathWorks, Natick, Massachusetts, USA). Signals with embedded artifacts were exported in CSV format, and further analyses and calculations were done in Python (version 3.8.8, Python Software Foundation, Wilmington, Delaware, USA). The whole data processing is depicted in Fig. 2.

Short-time Fourier transform was performed on the signals with different artifacts to detect the changes in the frequency domain caused by the embedded artifacts. A 5-second window with 50% overlap was used to calculate the short-time Fourier transform (STFT) because it can be assumed that only minor changes in heart rate occur during this interval. Based on the observation of the STFT of the segments, three rules for artifact identification were set.

First, the dominant frequency component of the power spectrum calculated in the frequency range of 0.2–20 Hz must be within 0.5–3.33 Hz band, which corresponds to the fundamental harmonic of the heart rate of 30–200 min^{-1} as the main component of the ABP signal. The segment was identified as artifact-containing if the dominant frequency was outside the 0.5–3.33 Hz range.

Second, the standardized power spectrum calculated in the 0.2–1 Hz frequency range was further analyzed to find low-frequency artifacts in segments with a preserved pulsating signal. If the value of the standardized power spectrum exceeded fifty percent of the maximum value of the power spectrum calculated within a 10-minute window, it was classified as an artifact.

Third, the value of the second harmonic of the dominant frequency component within the individual power spectrum segments was calculated. If this value

Lekar a technika – Clinician and Technology 2024, vol. 54(2), pp. 63–72, DOI: 10.14311/CTJ.2024.2.05
ISSN 0301-5491 (Print), ISSN 2336-5552 (Online)

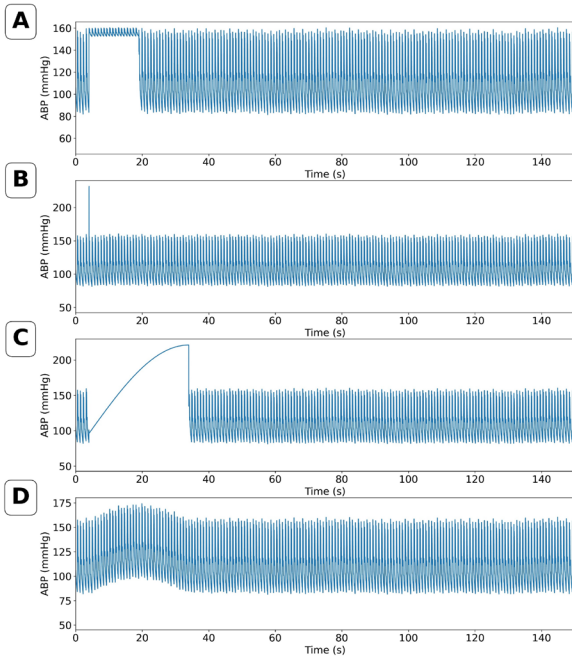

Fig. 1: Four types of modeled artifacts, each inserted at the 4th second into the ABP waveform. A) An example of a rectangular artifact (15 s long, 50% amplitude rise). B) Fast impulse (0.04 s long, 125% amplitude rise). C) An example of a sawtooth artifact (15 s long, 50% amplitude rise). D) An example of a baseline drift artifact (30 s long, 15% amplitude rise).

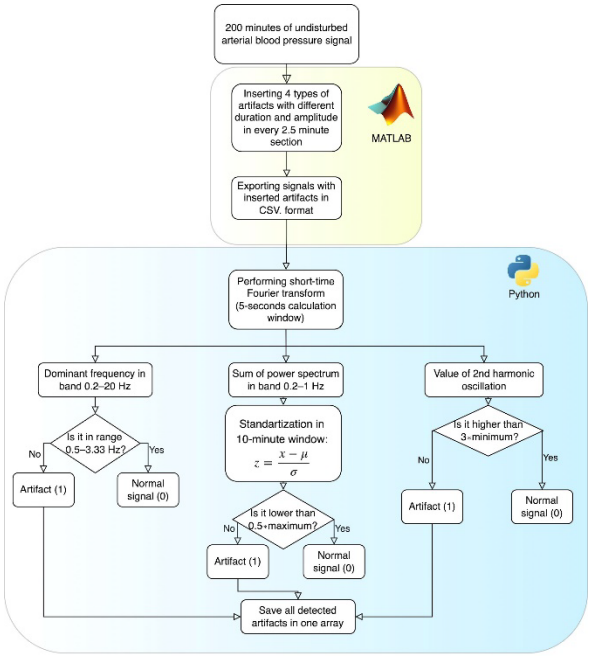

Fig. 2: Flowchart depicting the data processing and artifact identification in three rules. Each data segment had to pass all three rules to be labeled artifact-free. The standardized value (z) is standardly calculated from the raw value (x), mean (μ), and standard deviation (σ).

was less than three times the minimum value of the power spectra calculated within the 10-minute window, it was identified as an artifact.

Table 1: Parameters of simulated artifacts [3].

Type of artifact	Duration (s)	Amplitude rise (%)
Rectangular	4; 15; 30; 60	25; 50; 75; 100
Fast impulse	0.04	25; 50; 75; 100; 125
Sawtooth	30; 45; 90	30; 60
Baseline drift	15; 30; 60; 120	15; 30

If a segment passed all three rules, it was determined to be artifact-free; a positive finding in at least one of the rules identified the segment as artifact-containing.

Statistical analysis

Sensitivity and specificity were calculated to evaluate the performance of the detection algorithm. As true positive values, we used the number of inserted artifact points correctly labeled by the algorithm. Signal segments without inserted artifacts that were not marked by the algorithm as an artifact were considered true negatives.

Results

Four types of artifacts with different durations and amplitude rises were inserted into arterial blood pressure signals. An example of a rectangular artifact, its frequency analysis, and its detection by the algorithm is depicted in Fig. 3. Examples of other types of artifacts can be found in Fig. S1–S3 in Supplementary Materials.

Table 2 presents the sensitivity and specificity calculated for particular types of artifacts. A more detailed view of the differences among different artifacts' amplitudes and durations can be found in Tables S1 and S2 in Supplementary Materials. The sensitivity increases with higher amplitudes of artifacts and in longer rectangle and saw tooth artifacts. For example, the sensitivity for the 30-s saw tooth artifact is 93.37% and for the 90-s artifact is 96.84%. However, the sensitivity for the 4-s rectangle artifact is 99.53% but drops to 86.70% for the 15-s rectangle, 91.73% for the 30-s, and 95.46% for the 60-s rectangle. On the contrary, the sensitivity of detection of baseline drift declines with increasing artifact length (7.05% for 15 s to 2.18% for 120 s). Due to the 0% sensitivity of the fast impulse artifacts, it was not added to the Tables S1 and S2 in Supplementary Materials.

The false positive rate was 0.00% for all artifact types, durations, and amplitudes.

Lekar a technika – Clinician and Technology 2024, vol. 54(2), pp. 63–72, DOI: 10.14311/CTJ.2024.2.05
ISSN 0301-5491 (Print), ISSN 2336-5552 (Online)

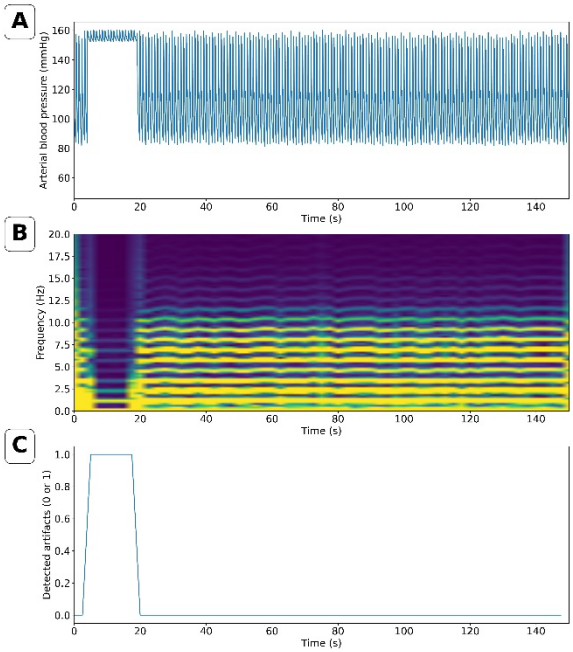

Fig. 3: An example of a modeled rectangular artifact with 15-s duration and 50% amplitude rise inserted into an undisturbed ABP signal. A) ABP signal with inserted artifact; B) Artifact frequency analysis; C) Detection of the artifact as an algorithm output.

Table 2: Results of detection for each type of simulated artifact

Type of artifact	Sensitivity (%)	Specificity (%)
Rectangular	93.35	99.34
Fast impulse	0.00	99.82
Sawtooth	94.83	99.14
Baseline drift	5.02	98.78

Discussion

The main finding of this study is that the algorithm based on short-time Fourier transform reliably detected rectangular and sawtooth artifacts in arterial blood pressure signals, with sensitivities of 93.35% and 94.83%, respectively, and specificities exceeding 99% for both artifact types. Baseline drifts were detected with a low sensitivity of 5.02%, and fast impulses were not detected.

The proposed algorithm presents a novel approach that utilizes the time-varying frequency components of the ABP signal to achieve faster artifact detection. Specifically, a short-time Fourier transform is employed to observe changes in the frequency spectrum over time (Fig. 3B).

To our knowledge, this study is the first to use solely STFT for artifact detection in ABP signals, offering a simpler, more computationally efficient alternative to complex machine learning approaches, and directly addressing the need for real-time, accurate artifact detection in clinical settings. Besides employment in studies on electroencephalography (EEG) signals [17, 18], STFT images have been used as an input for deep learning methods for artifact detection in photoplethysmography signals by Chen et al. [19].

In ABP signal artifact detection, STFT was partly applied by Rinehart et al. [14]. Their algorithm was mainly based on machine learning (ML) protocol; however, in data preparation, they utilized a fast-Fourier transform based convolution lowpass filter with a cutoff frequency of 2.5 Hz and transition band 30 Hz. Subsequently, the data underwent a beat-detection algorithm, including the Fourier transform, to detect the dominant time constant. This approach is similar to the first rule in our algorithm; however, we added the other two rules to detect different types of artifacts better.

We find the use of STFT alone advantageous because of its straightforwardness, especially compared to machine learning approaches. Moreover, a simpler algorithm can be less computationally demanding, which might be important for online data analysis. Son et al. [8] measured the CPU time for their deep belief network method, and the increase was twofold compared to a non-machine-learning algorithm but still insignificant in practical application. Additionally, the ML detection tools are significantly reliant on the input of large amounts of data annotated by experienced physicians with known great inter- and intraindividual variability [20, 21]. Compared to that, the performance of the presented algorithm based on the STFT is determined by tuning the parameters, and considerable testing on clinical data is inevitable.

In our previous study [3], we found that the effect of artifacts on the pressure reactivity index could vary depending on their type, duration, and amplitude rise. The most common artifact—fast impulse—had a minimal effect as the calculation of PRx involves a filtering process in which both input pressure waveforms (intracranial and arterial blood pressure) are averaged with a 10-second window. This averaging acts as a low-pass filter and suppresses short artifacts such as fast impulses. The same minimal effect was observed for baseline drift; moreover, the origin of this particular artifact is questionable and, in some cases, might not be of an artificial origin. Therefore, during detection algorithm development, we focused mainly on detecting rectangular and saw tooth artifacts. In these artifacts, we achieved sensitivity and specificity of over 90% (Table 2), which is the general aim of algorithm tuning in similar studies [8, 9]. The sensitivity was low for baseline drift, but the specificity was above 90%, so identifying signals with artifacts was preserved.

However, for the rectangle shape, the detection sensitivity of 15-s long artifact (86.70%) is worse than that for 4 s (99.53%). The authors speculate that there

Lekar a technika – Clinician and Technology 2024, vol. 54(2), pp. 63–72, DOI: 10.14311/CTJ.2024.2.05
ISSN 0301-5491 (Print), ISSN 2336-5552 (Online)

can be an additional effect of the designed algorithm. The way the proposed algorithm is designed may lead to greater sensitivity to the ratio of the length of the computational window to the length of the embedded artifact. The algorithm especially recognizes the sharp edges in the analyzed signal, but the middle parts of rectangular artifacts may be detected with less sensitivity in some cases. The third rule assessing the value of the second harmonic of the dominant frequency was used for improvement of detection of these middle parts.

We do not see as a major issue the fact that the algorithm lacks the ability to detect the fast impulse. The modeled fast impulse is only 0.04 s long, so its duration is much shorter than the time resolution capability of the detection algorithm. Moreover, it has an insignificant effect on further analyses (like PRx [3]), and for higher amplitudes, it can be easily removed by simple filters, including using the averaging incorporated in the PRx calculation.

Our study has several limitations. Firstly, we acknowledge that the presented algorithm may encounter challenges in identifying some modeled artifacts. We focused the detection algorithm development on the artifacts with larger under-curve areas with a more pronounced effect on PRx and other secondary calculations and signal processing. In rectangular artifacts, the problem can be attributed to outliers in the frequency spectrum that may hinder the accurate detection of these artifacts. Furthermore, our algorithm was primarily designed and tested in controlled settings using modeled artifacts on ABP waveforms within a tight MAP range of 90 ± 5 mmHg and in the absence of arrhythmias. The subsequent crucial phase has to involve further testing and refining the algorithm using real clinical data, particularly when faced with varied pathophysiological conditions.

Moreover, the algorithm is intended for artifact detection but does not solve the problem of management of the artifact-containing waveform. On the other hand, in many cases, the clinician does not need a substitute for an artifact-polluted physiological parameter, whereas they need to know that the presented value itself or as an input for a secondary parameter calculation is burdened with inaccuracy.

The algorithm development and testing have been limited to four modeled artifacts so far, and for example, large complex artifacts were not included in the analysis. However, this approach has been used in other studies as well, besides other reasons due to a lack of gold standard for artifact annotation and frequent interindividual disagreement among annotators [20, 21]. Li et al. [5] also modeled artifacts of different shapes in Matlab software and used them to evaluate their artifact detection tool. Rinehart et al. [14] developed their algorithm on induced artifacts of low and high positions of pressure transducer and damped signal; other artifacts like arterial line flushes and motor-evoked potential monitoring were filtered out. Subsequent evaluation of the detection of real-life artifacts is an essential next step. Future development should focus on refining the algorithm to better handle complex artifacts and integrating it into signal recording software, with the ultimate goal of embedding it into bedside monitors for real-time clinical use.

Conclusion

This study successfully demonstrates the potential of a short-time Fourier transform-based algorithm in enhancing the detection of artifacts in arterial blood pressure signals. Although this algorithm shows promise in identifying ABP artifacts, its training has been limited to simulated data. The high sensitivity and specificity observed for clinically significant rectangular and sawtooth artifacts highlight the algorithm's potential to improve the accuracy of secondary calculations, such as PRx, in neurocritical care. Continued development and testing in diverse clinical conditions will be crucial to fully realize the algorithm's potential in real-time clinical monitoring.

Acknowledgement

The study was supported by the grant SGS22/202/OHK4/3T/17 and SGS23/198/OHK4/3T/17.

Lekar a technika – Clinician and Technology 2024, vol. 54(2), pp. 63–72, DOI: 10.14311/CTJ.2024.2.05
ISSN 0301-5491 (Print), ISSN 2336-5552 (Online)

Supplementary Materials

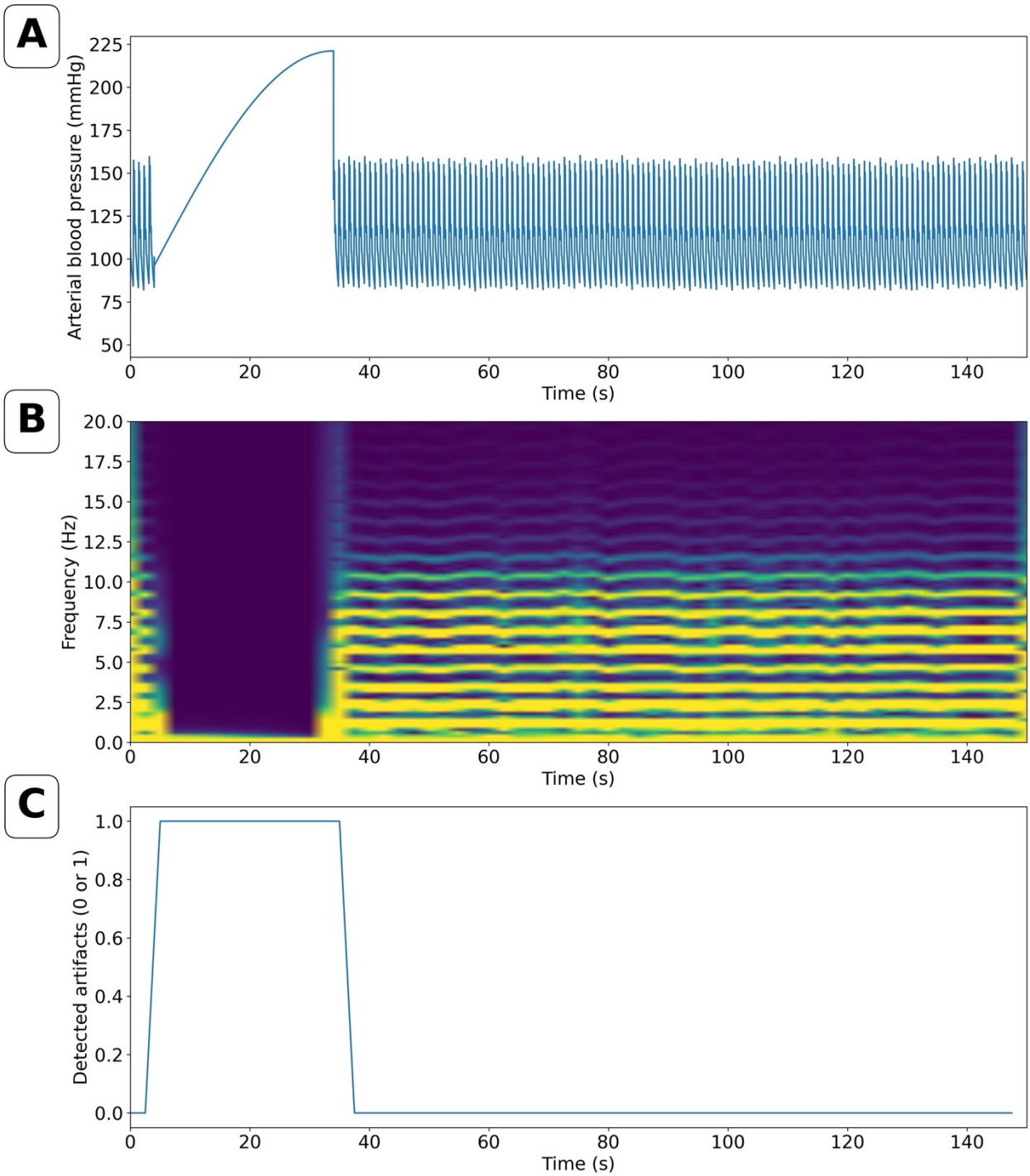

Fig. S1: An example of a modeled saw tooth artifact with duration of 15 s and 50% amplitude rise inserted into an undisturbed ABP signal. A) ABP signal with inserted artifact; B) Artifact frequency analysis; C) Detection of the artifact as an algorithm output.

Lekar a technika – Clinician and Technology 2024, vol. 54(2), pp. 63–72, DOI: 10.14311/CTJ.2024.2.05
ISSN 0301-5491 (Print), ISSN 2336-5552 (Online)

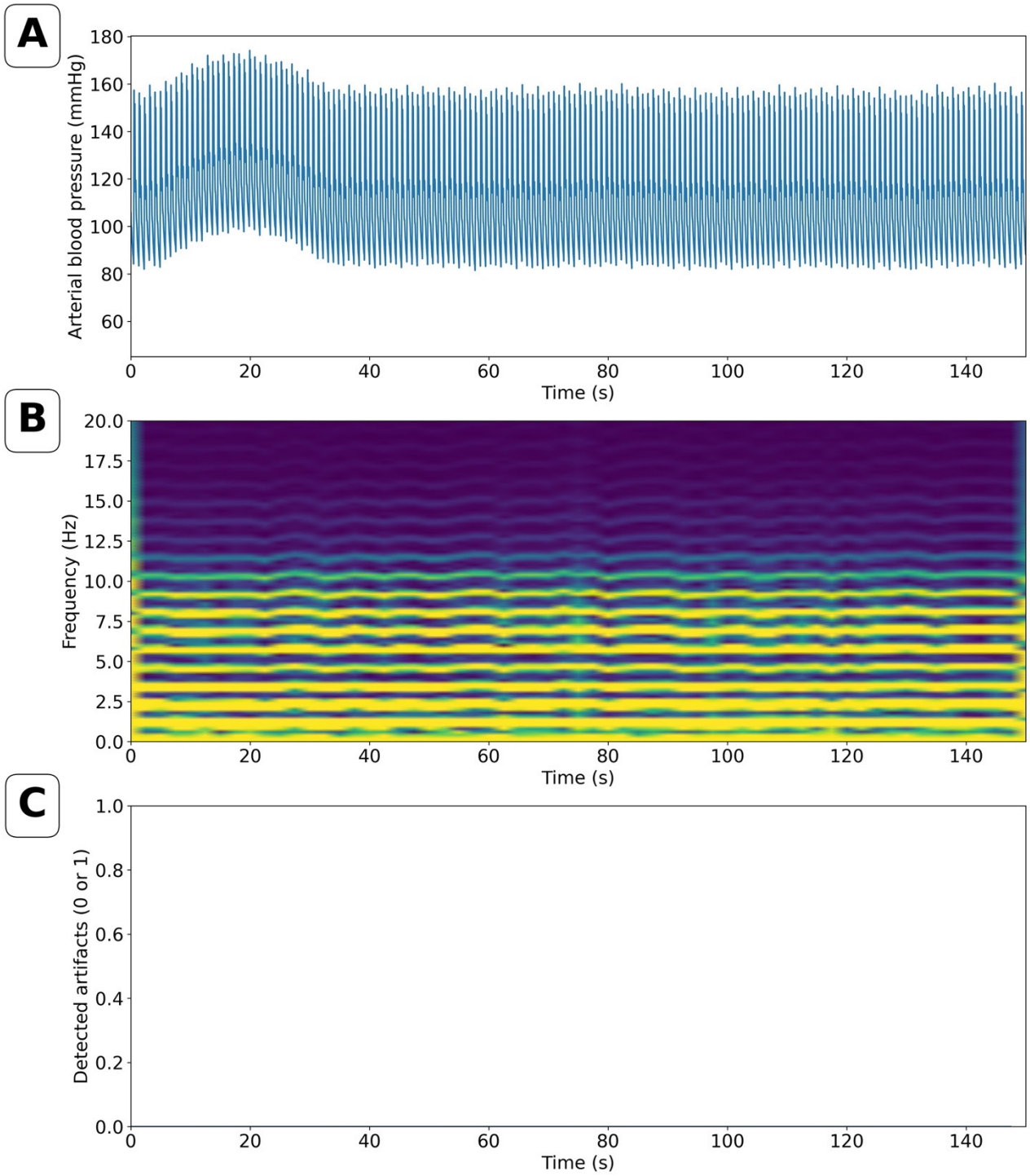

Fig. S2: An example of a modeled baseline drift artifact with duration of 30 s and 15% amplitude rise inserted into an undisturbed ABP signal. A) ABP signal with inserted artifact; B) Artifact frequency analysis; C) Detection of the artifact as an algorithm output.

Lekar a technika – Clinician and Technology 2024, vol. 54(2), pp. 63–72, DOI: 10.14311/CTJ.2024.2.05
ISSN 0301-5491 (Print), ISSN 2336-5552 (Online)

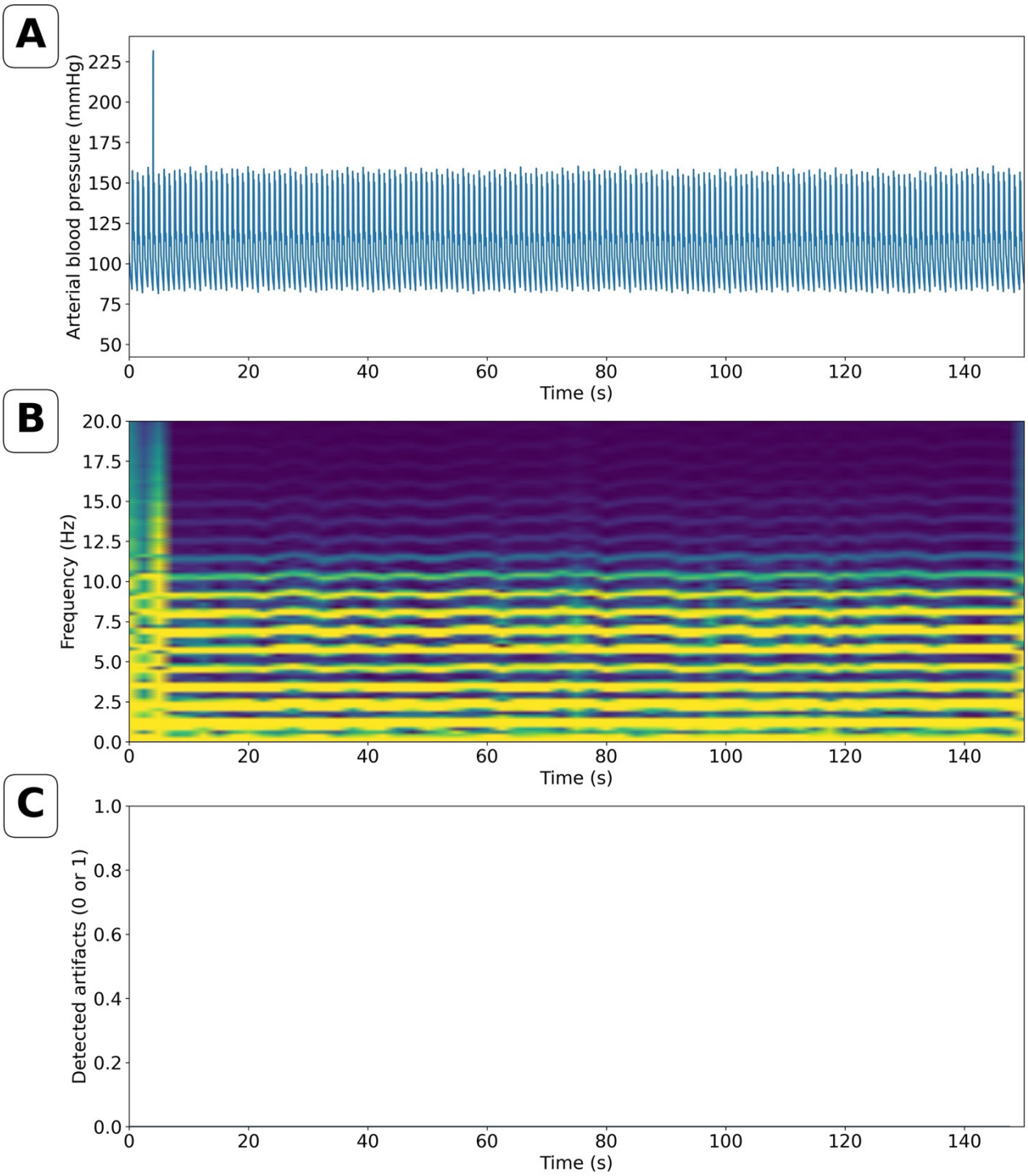

Fig. S3: An example of a modeled fast impulse artifact with duration of 0.04 s and 125% amplitude rise inserted into an undisturbed ABP signal. A) ABP signal with inserted artifact; B) Artifact frequency analysis; C) Detection of the artifact as an algorithm output.

Lekar a technika – Clinician and Technology 2024, vol. 54(2), pp. 63–72, DOI: 10.14311/CTJ.2024.2.05
ISSN 0301-5491 (Print), ISSN 2336-5552 (Online)

Table S1: Comparison of the algorithm's sensitivity and specificity (%) depending on the modeled artifact's duration. The results are an average for all amplitudes of the given type of artifact.

Rectangle	**Saw tooth**	**Baseline drift**
4 s	**30 s**	**15 s**
Sensitivity 99.53	Sensitivity 93.37	Sensitivity 7.05
Specificity 99.45	Specificity 99.39	Specificity 99.42
15 s	**45 s**	**30 s**
Sensitivity 86.70	Sensitivity 94.28	Sensitivity 6.35
Specificity 99.42	Specificity 99.29	Specificity 99.34
30 s	**90 s**	**60 s**
Sensitivity 91.73	Sensitivity 96.84	Sensitivity 4.48
Specificity 99.35	Specificity 98.74	Specificity 99.16
60 s		**120 s**
Sensitivity 95.46		Sensitivity 2.18
Specificity 99.15		Specificity 97.21

Table S2: Comparison of sensitivity and specificity (%) of the algorithm depending on the amplitude rise of the modeled artifact. The results are an average for all durations of the given type of artifact.

Rectangle	**Saw tooth**	**Baseline drift**
25%	**30%**	**15%**
Sensitivity 87.31	Sensitivity 94.03	Sensitivity 0.89
Specificity 99.35	Specificity 99.14	Specificity 98.78
50%	**60%**	**30%**
Sensitivity 94.31	Sensitivity 95.62	Sensitivity 9.14
Specificity 99.35	Specificity 99.14	Specificity 98.79
75%		
Sensitivity 95.39		
Specificity 99.38		
100%		
Sensitivity 96.40		
Specificity 99.29		

Lekar a technika – Clinician and Technology 2024, vol. 54(2), pp. 63–72, DOI: 10.14311/CTJ.2024.2.05
ISSN 0301-5491 (Print), ISSN 2336-5552 (Online)

References

[1] Tas J, Czosnyka M, Van Der Horst IC, Park S, Van Heugten C, Sekhon M, et al. Cerebral multimodality monitoring in adult neurocritical care patients with acute brain injury: A narrative review. Frontiers in Physiology. 2022 Dec 1;13:1071161. DOI: 10.3389/fphys.2022.1071161

[2] Czosnyka M, Smielewski P, Kirkpatrick P, Laing RJ, Menon D, Pickard JD. Continuous Assessment of the Cerebral Vasomotor Reactivity in Head Injury. Neurosurgery 1997 Jul;41(1):11–9.

[3] Rozanek M, Skola J, Horakova L, Trukhan V. Effect of artifacts upon the pressure reactivity index. Scientific Reports. 2022 Sep 6;12(1):15131. DOI: 10.1038/s41598-022-19101-y

[4] Saugel B, Kouz K, Meidert AS, Schulte-Uentrop L, Romagnoli S. How to measure blood pressure using an arterial catheter: a systematic 5-step approach. Critical Care. 2020 Apr 24;24:1–10. DOI: 10.1186/s13054-020-02859-w

[5] Li Q, Mark RG, Clifford GD. Artificial arterial blood pressure artifact models and an evaluation of a robust blood pressure and heart rate estimator. BioMedical Engineering OnLine. 2009 Jul 8;8:1–15. DOI: 10.1186/1475-925X-8-13

[6] Rotariu C, Pasarica A, Costin H, Adochiei F, Ciobotariu R. Telemedicine system for remote blood pressure and heart rate monitoring. 2011 E-Health and Bioengineering Conference (EHB); 2011 Nov 24–26; Iasi, Romania. IEEE; 2011.

[7] Zong W, Moody GB, Mark RG. Reduction of false arterial blood pressure alarms using signal quality assessement and relationships between the electrocardiogram and arterial blood pressure. Medical and Biological Engineering and Computing. 2004 Sep;42:698–706. DOI: 10.1007/BF02347553

[8] Son Y, Lee SB, Kim H, Song ES, Huh H, Czosnyka M, et al. Automated artifact elimination of physiological signals using a deep belief network: An application for continuously measured arterial blood pressure waveforms. Information Sciences. 2018 Aug;456:145–58. DOI: 10.1016/j.ins.2018.05.018

[9] Khan JM, Maslove DM, Boyd JG. Optimized Arterial Line Artifact Identification Algorithm Cleans High-Frequency Arterial Line Data With High Accuracy in Critically Ill Patients. Critical Care Explorations. 2022 Dec;4(12):e0814. DOI: 10.1097/CCE.0000000000000814

[10] Imhoff M, Bauer M, Gather U, Löhlein D. Statistical pattern detection in univariate time series of intensive care on-line monitoring data. Intensive Care Medicine. 1998 Dec;24:1305–14. DOI: 10.1007/s001340050767

[11] Pasma W, Wesselink EM, Van Buuren S, De Graaff JC, Van Klei WA. Artifacts annotations in anesthesia blood pressure data by man and machine. Journal of Clinical Monitoring and Computing. 2021 Aug 12;35:259–67. DOI: 10.1007/s10877-020-00574-z

[12] Du CH, Glick D, Tung A. Error-checking intraoperative arterial line blood pressures. Journal of Clinical Monitoring and Computing. 2019 Jun 5;33:407–12. DOI: 10.1007/s10877-018-0167-7

[13] Lee SB, Kim H, Kim YT, Zeiler FA, Smielewski P, Czosnyka M, et al. Artifact removal from neurophysiological signals: impact on intracranial and arterial pressure monitoring in traumatic brain injury. Journal of Neurosurgery. 2019 May 10;132(6):1952–60. DOI: 10.3171/2019.2.JNS182260

[14] Rinehart J, Tang J, Nam J, Sha S, Mensah P, Maxwell H, et al. Detection of arterial pressure waveform error using machine learning trained algorithms. Journal of Clinical Monitoring and Computing. 2022 Feb 1;36:227–37. DOI: 10.1007/s10877-020-00642-4

[15] Sun JX, Reisner AT, Mark RG. A signal abnormality index for arterial blood pressure waveforms. 2006 Computers in Cardiology; 2006 Sep 17–20; Valencia, Spain. IEEE; 2006.

[16] Zhang P, Liu J, Wu X, Liu X, Gao Q. A Novel Feature Extraction Method for Signal Quality Assessment of Arterial Blood Pressure for Monitoring Cerebral Autoregulation. 2010 4th International Conference on Bioinformatics and Biomedical Engineering; 2010 Jun 18–20; Chengdu, China. IEEE; 2010. DOI: 10.1109/ICBBE.2010.5515739

[17] Yücelbaş C, Yücelbaş Ş, Özşen S, Tezel G, Küçüktürk S, Yosunkaya Ş. Automatic detection of sleep spindles with the use of STFT, EMD and DWT methods. Neural Computing and Applications. 2018;29:17–33. DOI: 10.1007/s00521-016-2445-y

[18] Taherisadr M, Dehzangi O, Parsaei H. Single Channel EEG Artifact Identification Using Two-Dimensional Multi-Resolution Analysis. Sensors. 2017 Dec 13;17(12):2895. DOI: 10.3390/s17122895

[19] Chen J, Sun K, Sun Y, Li X. Signal Quality Assessment of PPG Signals using STFT Time-Frequency Spectra and Deep Learning Approaches. 2021 43rd Annual International Conference of the IEEE Engineering in Medicine & Biology Society (EMBC); 2021 Nov 1–5; Mexico. IEEE; 2021. DOI: 10.1109/EMBC46164.2021.9630758

[20] Cunningham S, Symon AG, McIntosh N. The practical management of artifact in computerised physiological data. Journal of Clinical Monitoring and Computing. 1994 Nov;11:211–6. DOI: 10.1007/BF01139872

[21] Verduijn M, Peek N, De Keizer NF, Van Lieshout EJ, De Pont AC, Schultz MJ, et al. Individual and Joint Expert Judgments as Reference Standards in Artifact Detection. Journal of the American Medical Informatics Association. 2008 Mar;15(2):227–34. DOI: 10.1197/jamia.M2493

Ing. Valeriia Trukhan
Department of Biomedical Technology
Faculty of Biomedical Engineering
Czech Technical University in Prague
nám. Sítná 3105, CZ-272 01 Kladno

E-mail: trukhval@fbmi.cvut.cz
Phone: +420 778 891 869

Lekar a technika – Clinician and Technology 2024, vol. 54(2), pp. 63–72, DOI: 10.14311/CTJ.2024.2.05
ISSN 0301-5491 (Print), ISSN 2336-5552 (Online)